

Forum

Solution-Based Synthetic Strategies for 1-D Nanostructures

Xun Wang and Yadong Li*

Department of Chemistry, Tsinghua University, Beijing 100084, People's Republic of China

Received October 31, 2005

One-dimensional (1-D) nanostructures of materials have received great research attention because of their unique photochemistry, photophysical, and electron-transport properties different from those of bulky or nanoparticle materials. One of the main challenges in this field is how to precisely control the sizes, dimensionalities, compositions, and crystal structures of materials in nanoscale. This review summarizes the recent progress in the solution-based routes to prepare 1-D nanostructures, highlighting the contribution from this laboratory. Crystal structure as one of the inherent factors that may determine the growth behavior of the nanocrystals is emphasized in this paper. Particularly compounds with layered structures or anisotropic crystal structures are given special attention in the controlled growth of 1-D nanostructures. This review aims to present a relatively general understanding of the correlation between the crystal structure and growth behavior of materials under solution-based conditions and show how to choose appropriate conditions for the growth of 1-D nanostructures.

Introduction

Since the discovery of the C nanotubes,¹ one-dimensional (1-D) nanostructures of materials have received great research attention because of their unique photochemistry, photophysical, and electron-transport properties different from those of bulky or nanoparticle materials.^{2–21} On the basis of

well-defined 1-D nanostructures and/or 1-D arrays, many new and promising fields have been established, including nanofabrication,^{11–14} nanodevices,^{15–20} nanobiology,²¹ nanocatalysis,²² etc.

Among all of the challenges in 1-D fields, the first yet most fundamental one would be how to control the growth of 1-D nanostructures. The essence of 1-D nanostructure formation is about crystallization. The evolution of a solid from a vapor, liquid, or solid phase involved nucleation and growth. As for 1-D nanostructures, the growth involves the breaking of crystal symmetry and is quite different from the general concept of crystal growth, so emphasis should be paid to the ways that the building blocks will be arranged to ensure the anisotropic growth of the nanocrystals. For

* To whom correspondence should be addressed. E-mail: ydli@mail.tsinghua.edu.cn.

- Iijima, S. *Nature* **1991**, *354*, 56–58.
- Tenne, R.; Margulis, L.; Genut, M.; Hodes, G. *Nature* **1992**, *360*, 444–446.
- Trentler, T. J.; Hickman, K. M.; Geol, S. C.; Viano, A. M.; Gibbons, P. C.; Buhro, W. E. *Science* **1995**, *270*, 1791–1794.
- Dai, H. J.; Wong, E. W.; Lu, Y. Z.; Fan, S. S.; Lieber, C. M. *Nature* **1995**, *375*, 769–772.
- Han, W. Q.; Fan, S. S.; Li, Q. Q.; Hu, Y. D. *Science* **1997**, *277*, 1287–1289.
- Morales, A. M.; Lieber, C. M. *Science* **1998**, *279*, 208–211.
- Peng, X. G.; Manna, L.; Yang, W. D.; Wickham, J.; Scher, E.; Kadavanich, A.; Alivisatos, A. P. *Nature* **2000**, *404*, 59–61.
- Duan, X. F.; Lieber, C. M. *Adv. Mater.* **2000**, *12*, 298–302.
- Pan, Z. W.; Dai, Z. R.; Wang, Z. L. *Science* **2001**, *291*, 1947–1949.
- Huang, M. H.; Wu, Y. Y.; Feick, H.; Yang, P. D.; et al. *Adv. Mater.* **2001**, *13*, 113–116.
- Goldberger, J.; He, R. R.; Zhang, Y. F.; Yang, P. D.; et al. *Nature* **2003**, *422*, 599–602.
- Wu, Y. Y.; Fan, R.; Yang, P. D. *Nano Lett.* **2002**, *2*, 83–86.
- Hu, J. T.; Odom, T. W.; Lieber, C. M. *Acc. Chem. Res.* **1999**, *32*, 435–445.
- Xia, Y. N.; Yang, P. D.; Sun, Y. G.; et al. *Adv. Mater.* **2003**, *15*, 353–389.

- Fan, S. S.; Chapline, M. G.; Franklin, N. R.; et al. *Science* **1999**, *283*, 512–514.
- Huang, M. H.; Mao, S.; Feick, H.; Yang, P. D.; et al. *Science* **2001**, *292*, 1897–1899.
- Duan, X. F.; Huang, Y.; Cui, Y.; Lieber, C. M.; et al. *Nature* **2001**, *409*, 66–69.
- Huang, Y.; Duan, X. F.; Cui, Y.; Lieber, C. M.; et al. *Science* **2001**, *294*, 1313–1317.
- Cui, Y.; Lieber, C. M. *Science* **2001**, *291*, 851–853.
- Huang, Y.; Duan, X. F.; Wei, Q. Q.; et al. *Science* **2001**, *291*, 630–633.
- Cui, Y.; Wei, Q. Q.; Park, H. K.; Lieber, C. M. *Science* **2001**, *293*, 1289–1292.
- Zhou, K. B.; Wang, X.; Sun, X. M.; Peng, Q.; Li, Y. D. *J. Catal.* **2005**, *229*, 206–212.

example, when AAO are adopted as templates, the nucleation and growth processes can be controlled to take place in the confined spaces and the nanostructures will follow the shapes and sizes of the original templates;¹¹ in a typical vapor/liquid/solid (VLS) growth process, when metal clusters are employed as catalysts, the absorption of the monomers and the subsequent chemical reaction and/or crystal growth processes can proceed with the liquid clusters as energetic favorable sites, which may provide the driving force for the anisotropic growth of the as-obtained 1-D nanostructures.⁸

Several techniques have been successfully applied in the synthesis of 1-D nanostructures, such as VLS growth process,^{6,8} thermal evaporation,^{11,16} reverse micelles,²³ a template-confined method,⁵ etc. Particularly, solution-based routes can usually provide gram-scale samples even in laboratory and thus can be expanded to the industrial scale in a much easier way once potential applications could be realized. So, it would be quite fundamental to investigate the general formation mechanism (especially the driving force in the nucleation or growth stage) of 1-D nanostructures under solution conditions. In this paper, we will briefly review recent progress in solution-based synthesis strategies for 1-D nanostructure materials, highlighting the contributions from this laboratory. Crystal structure as one of the inherent factors that may determine the growth behavior of the nanocrystals is emphasized, and particularly compounds with layered structures or anisotropic crystal structures are given special attention in that they are often found related to the growth of 1-D nanostructures, including nanowires and nanotubes. In most of the summarized cases, the use of surfactants was avoided to simplify the reaction systems (although in some reports appropriate capping reagents do assist the growth of 1-D nanostructures), which may give us a clearer picture on the decisive factors.

The whole review is divided into three parts: (I) solvothermal synthesis of II–VI nanorods: from a solvent coordination molecular template (SCMT) mechanism to an understanding of inorganic/organic-layered structures; (II) proposal of a rolling mechanism: from a natural/artificial layered structure to nanotubes/nanowires; (III) controlled growth of nanowires/nanorods based on anisotropic crystal structures. The first and second parts aim to show the picture of a rolling mechanism: from layered structures to nanowires and/or nanotubes. The first part summarizes the research progress in solvothermal synthesis of II–VI nanorods, the growth of which was first believed to follow a SCMT mechanism. However, subsequent research revealed the existence of inorganic/organic-layered structures as intermediates. These experimental results contribute greatly to a mechanism from layered structure to nanorods, which serve as the basic guidelines for the successive synthesis of nanotubes or nanowires via solution-based methods. In the second part, a series of our research progress on single-crystal nanotubes including Bi, sodium titanate, WS₂, silicates, rare-earth hydroxides, Mn₂P₂S₆, etc., is summarized to show the close relationship between layered structures and the forma-

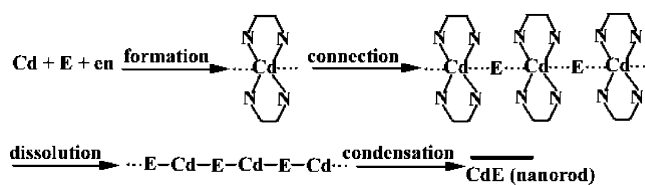


Figure 1. Scheme for a SCMT mechanism.²⁵

tion of nanotubes/nanowires. Most of the reported nanotubes have one character in common: layered structures in nature, which is regarded as the central point of a rolling mechanism. The third part deals with 1-D nanostructures of compounds with anisotropic crystal structures in nature.

This review aims to present a relatively general understanding of the correlation between the crystal structure and growth behavior of materials under solution-based conditions and show how to choose appropriate conditions for the growth of 1-D nanostructures.

Part I. Solvothermal Synthesis of II–VI Nanorods: From the SCMT Mechanism to an Understanding of Inorganic/Organic-Layered Structures

In the 1990s, the synthesis of nanowires/nanorods was not as effective as it is today. Although a template-confined method had been well established to get 1-D nanowires/nanorods, comparatively less success^{2–5} had been achieved in the controlled growth of high-quality single-crystal nanowires/nanorods, especially for II–VI semiconductors. In 1995, Buhro et al. developed a solution/liquid/solid method to synthesize III–V semiconductor nanowires. In 1998, Morales and Lieber reported the synthesis of Si nanowires via laser ablation,⁶ which was then developed to prepare II–VI semiconductor nanowires in 2000.⁸ In 1998, Li et al. found a solvothermal synthetic route to get II–VI nanorods²⁴ and provided a new strategy for II–VI nanorod synthesis.^{24,25}

The anisotropic growth of II–VI semiconductors was achieved through the direct reaction of metal powder and sulfur in ethylenediamine. It was also found that other solvents such as water and pyridine did not facilitate the growth of these nanorods. Ethylenediamine seemed to be crucial for the formation of 1-D nanorods or nanowires of these materials, and a SCMT mechanism was then proposed with an emphasis on the role of the ethylenediamine molecule in assisting the anisotropic crystal growth.

In a typical SCMT process, ethylenediamine acted as a structure-directing molecule that was incorporated into the inorganic framework first and then escaped from it to form nanocrystallites with desired morphologies (Figure 1). Some experimental results and reported data did support this assumption.^{24,25} At room temperature, metal Cd powder can react with a sulfur ethylenediamine solution. X-ray diffraction (XRD) analysis showed that the obtained white powder was neither CdS nor Cd but was the complex of $[\text{Cd}(\text{en})_2]^{2+}$, which was confirmed by IR spectroscopy. With an increase

(24) Li, Y. D.; Liao, H. W.; Qian, Y. T.; et al. *Chem. Mater.* **1998**, *10*, 2301–2303.

(25) Li, Y. D.; Liao, H. W.; Ding, Y.; et al. *Inorg. Chem.* **1999**, *38*, 1382–1387.

(23) Li, M.; Schnablegger, H.; Mann, S. *Nature* **1999**, *402*, 393–395.

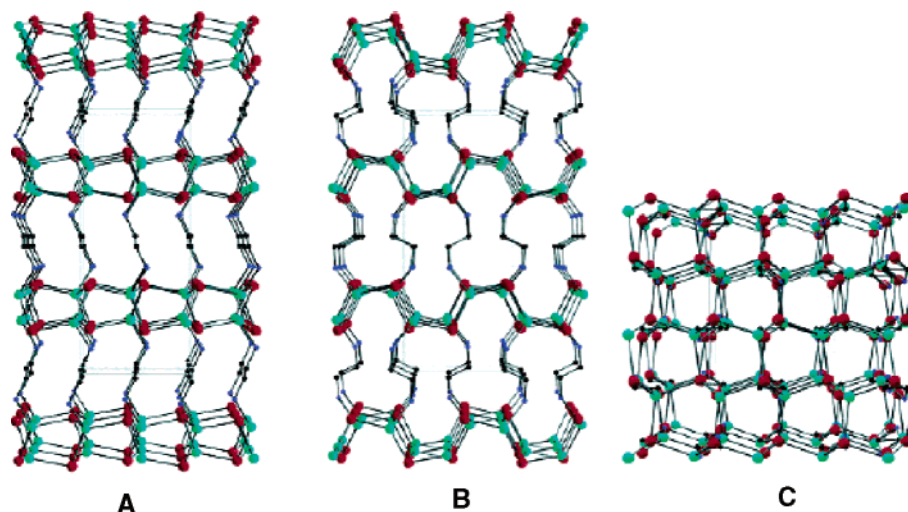


Figure 2. Structural views of CdSe.0.5en down the *a* (A), *b* (B), and *c* (C) axes of the orthorhombic cell. Red, cyan, blue, and black balls correspond to Cd, Se, N, and C atoms, respectively. H atoms are omitted for clarity.²⁷

of the temperature, the stability of the complexes decreased. At relatively elevated temperature (e.g., >120 °C), it was believed that S may connect the aforementioned complexes to form 1-D structural CdS nanorods and the volatile coordinated ligands were gradually lost. In this mechanism, during the process of CdS formation, it was proposed that this bidentate ligand complex served as an intermediate in the control of the CdS crystal growth. CdS was the result of the competition of the two reactions. In pyridine or diethylamine, the solvent molecules can also form complexes with Cd²⁺, but the stability of the complex was much lower than that of the former complex. The CdS formation reaction in these solvent systems was relatively easy, so the epitaxial growth of the CdS crystal was difficult to realize. However, no direct experimental evidence was obtained to support this idea, especially those concerning the exact formation process of these nanorods.

Then some inspiration resulted from the formation of ZnE.0.5en (E = S, Se; en = ethylenediamine) during the solvothermal treatment of appropriate Zn and S or Se sources in ethylenediamine.²⁶ They suggested that the formation of similar precursors might be the reason for the formation of CdE nanorods. In a subsequent work, crystallographic evidence for the formation of CdE.0.5en-layered precursors was reported,²⁷ which had been expected for the SCMT process. Detailed research was conducted on the role of ethylenediamine in the evolution from CdE.0.5en-layered precursors to CdE nanorods. On the basis of the crystal structures of these precursors and related experimental results, a tentative mechanism for the formation of CdE nanorods in ethylenediamine-mediated solvothermal synthesis was finally derived. Single-crystal XRD and powder XRD (PXRD), transmission electron microscopy (TEM), and thermogravimetric analysis (TGA) were employed for structural determination and morphology and composition analyses.

At appropriate solvothermal temperatures, a novel class of inorganic/organic-layered structures, CdE.0.5en (E = S, Se, Te; en = ethylenediamine), were obtained through reactions between elemental S, Se, or Te and Cd²⁺. These compounds contained atomic sheets of inorganic CdE frameworks spaced by ethylenediamine molecules, which served as bridged ligands between two Cd atoms in neighboring inorganic layers and also prevented these inorganic slabs from collapsing and condensing into the bulk CdE phase.

For example, structural solution from the single-crystal diffraction intensity data evidenced that CdSe.0.5en crystallized in the orthorhombic *Pbca* space group. This structure (Figure 2) could be viewed as a three-dimensional (3-D) network with two-dimensional (2-D) CdSe monolayers connected by bidentate ethylenediamine molecules. The CdSe monolayer contained mutually three-coordinated Cd and Se atoms. The inorganic CdSe slabs were then interconnected by ethylenediamine molecules with exclusively *trans* conformations bridged to Cd atoms in the neighboring layers. Therefore, the structure of CdSe.0.5en had interesting alternating semiconducting and insulating layers, which should exhibit a strong blue shift in optical absorption relative to the bulk-phased CdSe. This could be judged from the apparent color transition from dark purple to colorless when the 3-D CdSe inorganic network was split into monolayers by ethylenediamine molecules in the layered CdSe.0.5en compound and would be envisaged further by a diffuse-reflectance spectrum.

From the structural viewpoint, the essential mechanism for the formation of CdE nanorods in ethylenediamine-mediated solvothermal synthesis and the unique striated morphologies of the CdE products obtained through posthydrothermal treatment of the CdE.0.5en-layered precursors were revealed. The structure-selective crystallization of II–VI semiconductors in ethylenediamine under conditions of direct solvothermal synthesis or during the postconversion of the layered precursors was also explained on the basis of the similarity in atomic connectivity between the inorganic

(26) Deng, Z. X.; Wang, C.; Sun, X. M.; Li, Y. D. *Inorg. Chem.* **2002**, *41*, 869–873.

(27) Deng, Z. X.; Li, L. B.; Li, Y. D. *Inorg. Chem.* **2003**, *42*, 2331–2341.

Table 1. Representative Samples Concerning a Rolling Mechanism

nanowires/nanotubes via a rolling mechanism	natural layered structures	Bi nanotubes, ²⁹ silicate nanotubes, ³⁴ sodium titanate nanotubes, ³¹ MnO ₂ nanowires/nanotubes, ^{51–54} and Mn ₂ P ₂ S ₆ nanorods/nanotubes ³⁶
	nontypical layered structures organic/inorganic artificial layered structures	rare-earth nanowires/nanotubes and IF nanoparticles ^{61–65} WS ₂ nanotubes, ³³ W nanowires, ³⁷ WO _{3-x} nanowires, ³⁸ VO _x nanotubes, ³⁵ Bi nanotubes, ³⁰ Co nanowires, Cu nanowires, ³⁰ etc.

slabs in the precursors and those in wurtzite or zinc blende phases. A process from layered-structure intermediates to nanorods was thus described.²⁷

It is worth noting that the CdE_{0.5}en precursors, which possess strong quantum confinement effects resulting from their special inorganic/organic structures with alternating CdE and ethylenediamine layers, provide further possibilities of tailoring their electronic, magnetic, and optical properties through the structural modification of either the inorganic or organic components. On the basis of this idea, a series of inorganic/organic-layered-structure semiconductor single crystals, such as Ga₄Se₇(en)₂•(enH)₂ with an open framework, have been prepared.²⁸

Nevertheless, these layered-structure single-crystal intermediates do give us deep insight into the exact formation process of 1-D nanostructures. Different from the reported VLS or template method, it emphasizes the effect of the crystal structures on the evolution of morphologies. This crystallographic understanding also is in accordance with our assumption on the formation of 1-D nanostructures via a rolling mechanism.

Part II. Proposal of a Rolling Mechanism: From a Natural/Artificial Layered Structure to Nanotubes/Nanowires

Natural phenomena give us many inspirations; a piece of foliage or a piece of wet paper curls naturally during its drying process. If appropriate actions are applied, they will often form tubular structures. On the basis of a similar principle, if the interaction between neighboring layers could be reduced from the edges of the layer for a layered compound, tubular structures (or nanotubes) might also form through the rolling of these lamellar structures while keeping the interactions of in-layer atoms or molecules.

The concept of a rolling mechanism came into being during the investigation of the formation mechanism of II–VI semiconductors, and almost simultaneously it was verified by the successful preparation of Bi nanotubes,^{29,30} sodium titanate nanotubes/nanobelts,^{31,32} WS₂ nanotubes,³³ silicate nanotubes,³⁴ VO_x nanotubes,³⁵ Mn₂P₂S₆ nanotubes,³⁶ W³⁷ and WO_{3-x}³⁸ nanowires, etc. Its central point is that substances that possess lamellar structures might roll into nanotubes

under controlled experimental conditions. On the basis of this assumption, one can also deduce that (1) compounds that do not have layered structure will not form nanotubes without templates and (2) layered structures may serve as intermediates for the formation of nanowires/nanotubes (in the case of the above-mentioned II–VI nanorods, they stem from inorganic/organic-layered-structure intermediates). In recent years, our group has endeavored to explore new types of inorganic nanotubes/nanowires based on this rolling mechanism (Table 1). Great efforts have been paid to the design of favorable experimental conditions for the rolling of layered-structure compounds as well as the transformation of layered-structure intermediates into 1-D nanostructures.

1. Rolling Mechanism Based on Natural Layered Structures. This inspiration partly derived from the successful synthesis of C and other inorganic nanotubes, such as BxCyNz,³⁹ MS₂ (M = Mo, W, Nb, Ta, etc.),^{40,41} NiCl₂,⁴² and vanadium oxide (VO_x).⁴³ All of these compounds have layered structures in their bulk crystals, and the layers are held together mainly by weak van der Waals forces. It is believed that nanotubes are the thermodynamic stable forms of these compounds as a result of the existence of unsaturated bonds along the edges of 2-D layers. Layered structures are quite common in nature, such as Bi, black phosphorus, δ-MnO₂, sodium titanate, K₄Nb₆O₁₇, silicates, MoO₃, V₂O₅, various hydroxides, etc. Whether or not these layered structures can form nanotubes is an interesting topic in that it may help us to establish a direct relationship between the inherent crystal structure and their crystallographic morphologies. However, the interaction forces between layers are quite different for different layered structures. So, emphasis should be paid to the rational design of experimental conditions that would overcome the interaction between layers and thus facilitate the exfoliation and subsequent rolling process. Here several examples have been chosen to illustrate how to design solution-based synthetic routes to prepare nanotubes/nanowires from natural layered structures, including Bi, sodium titanate, silicates, δ-MnO₂, etc.

(28) Dong, Y. J.; Peng, Q.; Wang, R. J.; Li, Y. D. *Inorg. Chem.* **2003**, *42*, 1794–1796.

(29) Li, Y. D.; Wang, J. W.; Deng, Z. X.; et al. *J. Am. Chem. Soc.* **2001**, *123*, 9904–9905.

(30) Wang, J. W.; Li, Y. D. *Adv. Mater.* **2003**, *15*, 445–447.

(31) (a) Sun, X. M.; Li, Y. D. *Chem.—Eur. J.* **2003**, *9*, 2229–2238. (b) Sasaki, T.; Watanabe, M.; Komatsu, Y.; Fujiki, Y. *Inorg. Chem.* **1985**, *24*, 2265–2271.

(32) Sun, X. M.; Chen, X.; Li, Y. D. *Inorg. Chem.* **2002**, *41*, 4996–4498.

(33) Li, Y. D.; Li, X. L.; He, R. R.; et al. *J. Am. Chem. Soc.* **2002**, *124*, 1411–1416.

(34) (a) Wang, X.; Zhuang, J.; Chen, J.; Zhou, K. B.; Li, Y. D. *Angew. Chem., Int. Ed.* **2004**, *43*, 2017–2020. (b) Wang, X.; Zhuang, J.; Peng, Q.; Li, Y. D. *J. Solid State Chem.* **2005**, *178*, 2332–2338.

(35) Chen, X.; Sun, X. M.; Li, Y. D. *Inorg. Chem.* **2002**, *41*, 4524–4530.

(36) Li, C. H.; Wang, X.; Peng, Q.; Li, Y. D. *Inorg. Chem.* **2005**, *44*, 6641–6645.

(37) Li, Y. D.; Li, X. L.; Deng, Z. X.; et al. *Angew. Chem., Int. Ed.* **2002**, *41*, 333–335.

(38) Li, X. L.; Liu, J. F.; Li, Y. D. *Inorg. Chem.* **2003**, *42*, 921–924.

(39) Chopra, N. G.; Luyken, R. J.; Cherry, K.; Crespi, V. H.; Cohen, M. I.; Louie, S. G.; Zettl, A. *Science* **1995**, *269*, 966–967.

(40) Tenne, R. *Adv. Mater.* **1995**, *7*, 965–995.

(41) Tenne, R. *Chem.—Eur. J.* **2002**, *8*, 5297–5304.

(42) Hachohen, Y. R.; Grunbaum, E.; Sloan, J.; Hutchison, J. L.; Tenne, R. *Nature* **1998**, *395*, 336–337.

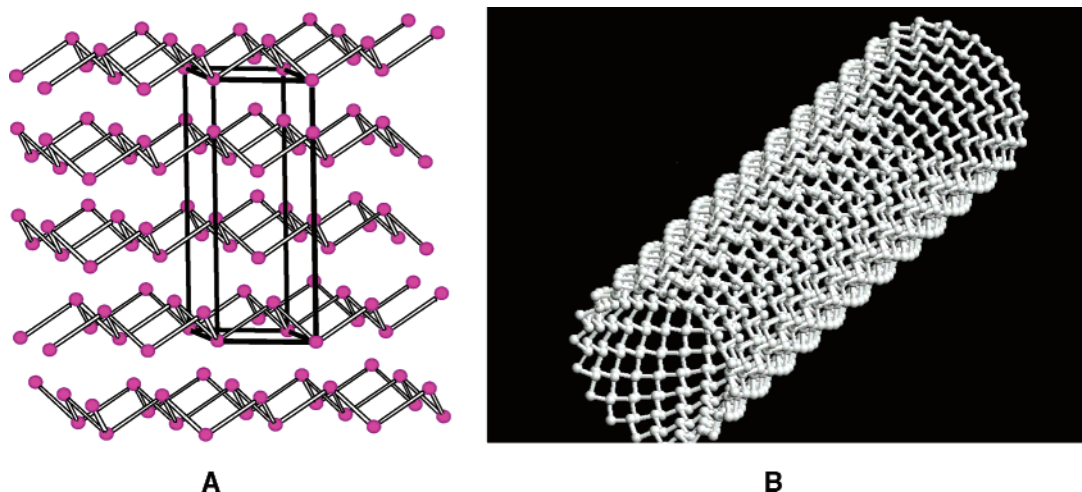


Figure 3. Structures of α -Bi (A) and Bi nanotubes (B).

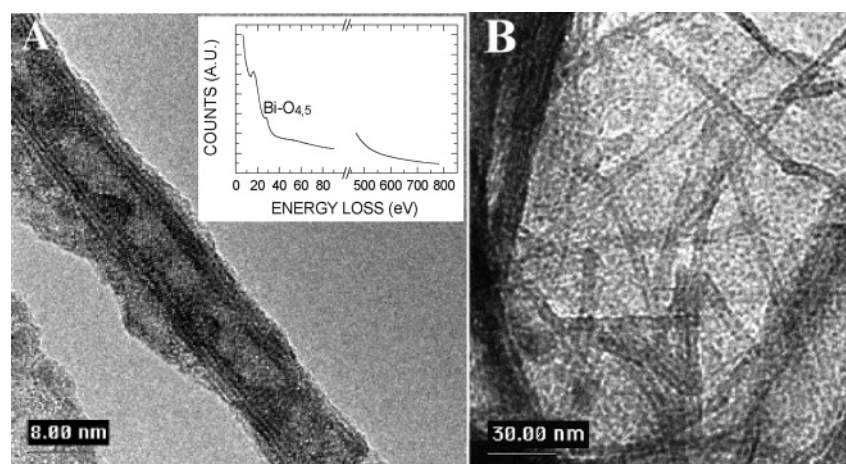


Figure 4. High-resolution TEM (HRTEM) images of an individual multiwall Bi nanotube. The inset in part a shows an electron energy loss spectroscopy spectra recorded on individual nanotubes.²⁹

Metallic Bi (R-Bi; Figure 3) has a pseudolayered structure very similar to that of rhombohedral graphite and black phosphorus.⁴⁴ In each layer, one Bi atom is connected with three other Bi atoms to form a trigonal pyramid. These pyramids further form a folded Bi layer by vertex sharing. The analogy between the layered structures of R-Bi and graphite/WS₂ indicates the possibility of the detachment of Bi molecular sheets and rolling into Bi nanotubes. However, owing to the relatively low melting point of Bi (271.3 °C), the synthesis of Bi nanotubes is much more difficult than that for C or MX₂ analogues. Most of the existing high-temperature approaches, such as arc-discharge evaporation, laser ablation, or chemical vapor deposition are inappropriate for the synthesis of Bi nanotubes.

Experimental results showed that the hydrothermal method was a rational synthetic mechanism for Bi nanotubes^{29,30} (Figure 4). Under hydrothermal conditions, Bi³⁺ could be reduced by N₂H₄·H₂O to form metal Bi, and the elevated temperature and pressure conditions would accelerate the movement of chemical species, which may contribute greatly

to the loosening of the layers from the edges. Under hydrothermal conditions, Bi nanotubes formed spontaneously without the aid of shape-regulating catalysts or templates. A significant portion (about 30%) of the sample dispersed on the TEM grids showed tubular structures, although other nanosheets were also observed. The existence of the sheetlike structures, as well as the tubular structures, was attributed to the layered feature in the crystal structure of rhombohedral Bi. The exfoliation and rolling process of the layers can be more effective if the artificial lamellar composite BiCl₄⁻/CTA⁺ (cetyltrimethylammonium) were adopted as a precursor³⁰ instead of Bi³⁺. Because of the intercalation of an organic component between layers, it was imaginable that the layer will become more flexible, and as a result, Bi nanotubes were obtained with much higher yield.

This proposed rolling mechanism has also been evidenced in the silicate series.³⁴ The basic unit of silicates is the (SiO₄) tetrahedron-shaped anionic group with a charge of 4⁻, which can be linked to each other in different modes and form as single units, double units, chains, sheets, rings, and framework structures. In the layered-structure subclass, hexagon rings of tetrahedrons are linked by shared O to other rings in a 2-D plane.⁴⁵ The Si/O ratio is generally 1:2.5 (or 2:5)

(43) Spahr, M. E.; Bitterli, P.; Nesper, R.; Müller, M.; Krumeich, F.; Nissen, H. U. *Angew. Chem., Int. Ed.* **1998**, *37*, 1263–1265.

(44) Wyckoff, R. W. G. *Crystal Structures*, 2nd ed.; Interscience: New York, 1973; Vol. 1, p 32.

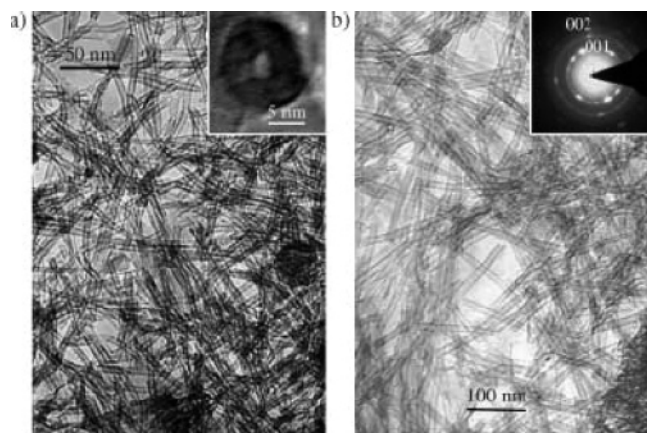


Figure 5. (a) TEM image of $\text{CuSiO}_3 \cdot 2\text{H}_2\text{O}$ nanotubes. (b) TEM image of $\text{Mg}_3\text{Si}_2\text{O}_5(\text{OH})_4$ nanotubes. Inset: electron diffraction patterns taken from a bundle of $\text{Mg}_3\text{Si}_2\text{O}_5(\text{OH})_4$.³⁴

because only one O is exclusively bonded to Si, and the other three are half-shared (1.5) to others. Pauling pioneered the study on the crystal structures of layered silicates including micas and chlorite. He predicted that if the two crystal faces of a constituent layer of a layered crystal were not equivalent, there would be a tendency for the layer to curve, with one face becoming concave and one convex. This tendency would, in general, not be overcome by the relatively weak force operative between adjacent layers.⁴⁶ It was believed that the growth of these silicate nanotubes was based on the asymmetry along the *c* axis of the layered metal silicates.

The synthesis of silicate nanotubes was based on a hydrothermal method in a mixed solution system. Although the silicates may have layered structures in nature, the direct reaction of metal ions and Na_2SiO_3 in water only resulted in irregular particles. All of these indicated that the formation of nanotubes may need some desirable conditions to facilitate the exfoliation process of the layers. Our experiments showed that a water/ethanol mixed solution was the optimal condition. The existence of ethanol may modulate the mobility of ion species.

All kinds of silicates could be prepared as uniform nanotube morphologies with open ends (Figure 5), which enabled them with possible applications in gas absorption/separation and catalysis fields. Because of the excellent ion-exchange characteristics of layered silicates, cations residing between the layers can be further replaced, which made these nanotubes ideal candidates as molecular sieves. The as-obtained nanotubes had tunable nanometer-scale pore sizes, narrow size distributions, and large Brunauer–Emmett–Teller surface areas and had shown a H_2 storage capacity of up to 1.8% at room temperature and an excellent catalytic oxidation performance at low-temperature range.³⁴

Silicate compounds are usually characteristic of affluent crystal structures and compositions. It still remains a difficult challenge to exactly control the growth behavior and morphology of the silicates. Nevertheless, this water/ethanol mixed solution synthetic route has shown some potential in

designed synthesis. Undoubtedly, the crystal structures of the final products are important factors that should be paid particular attention to, and in the case of silicate nanotubes, the underlying principle is the rolling mechanism from layered structures to nanotubes. Other distinctive structures are the chainlike silicates with $\text{Si}:\text{O} = 1:3$ when tetrahedra are connected to each other in a linear way, which may be favorable for the anisotropic growth. As stimulated by the successful synthesis of nanotubes from layered silicates, this water/ethanol hydrothermal route has been applied to the synthesis of silicate nanowires. By simple tuning of several parameters, such as temperature, concentration, ethanol/water ratios, etc., the crystal structure and growth behavior of nanocrystals can be easily modulated and several kinds of silicate nanowires, such as calcium silicates, strontium silicates, barium silicates, zinc silicates, cadmium silicates, etc., have been successfully prepared.

On the basis of our understanding of the proposed “rolling mechanism”, it is a premise of the spontaneous formation of single-crystalline nanotubes without the aid of templates that the compounds have either a natural or artificial lamellar structure. The layers are held together mainly by weak van der Waals forces for a typical layered-structure compound. The energy gap and rigidity would be lowered by adopting a tubular morphology. There exist many important metal oxides, such as TiO_2 , ZrO_2 , and Nb_2O_5 , that do not exhibit layered structures. The strong ionic interactions keep the metal cations and O anions together. So, they are stable against folding. Nanotubes from these nonlayered-structure materials generally require templates (e.g., C nanotubes⁴⁷ or anodic alumina oxide⁴⁸) to give spatial confinement, with the walls generally amorphous or semicrystalline.

However, the “rolling mechanism” was challenged by “ TiO_2 nanotubes”,^{49,50} which did not have layered structures yet was claimed to be prepared by nontemplate methods: alkaline hydrothermal treatment of titania or mixtures of $\text{TiO}_2/\text{SiO}_2$, followed by washing with water and a 0.1 M HCl aqueous solution. However, doubts remained concerning the formation and construction of these nanotubes.

Sun and Li optimized the synthetic procedure. A direct hydrothermal hydrolysis method was realized at 100–180 °C in a 5–10 M NaOH solution (Figure 6).³¹ Anatase TiO_2 was converted to large quantities of pure multiwall crystal sodium titanate nanotubes (with almost uniform inner diameters of 5 nm, outer diameters of 10 nm, and lengths of about 300 nm). Also, it was finally confirmed that these so-called “ TiO_2 nanotubes” were actually sodium titanate nanotubes (Figure 6). XRD, selected-area electron diffraction, energy-dispersive X-ray analysis (EDXA), thermal stability analysis, and ion-exchangeability analysis combined with magnetism measurements, photoluminescence, and UV/vis spectra were conducted to justify their structures. This

(45) Griffen, D. T. *Silicate Crystal Chemistry*; Oxford University Press: New York, 1992.

(46) Pauling, L. *Proc. Natl. Acad. Sci. U.S.A.* **1930**, *16*, 578–582

(47) Rao, C. N. R.; Satishkumar, B. C.; Govindaraj, A. *Chem. Commun.* **1997**, 1581–1582.

(48) Hoyer, P. *Langmuir* **1996**, *12*, 1411–1413.

(49) Kasuga, T.; Hiramatsu, M.; Hoson, A.; Sekino, T.; Niihara, K. *Langmuir* **1998**, *14*, 3160–3163.

(50) Kasuga, T.; Hiramatsu, M.; Hoson, A.; Sekino, T.; Niihara, K. *Adv. Mater.* **1999**, *11*, 1307–1311.

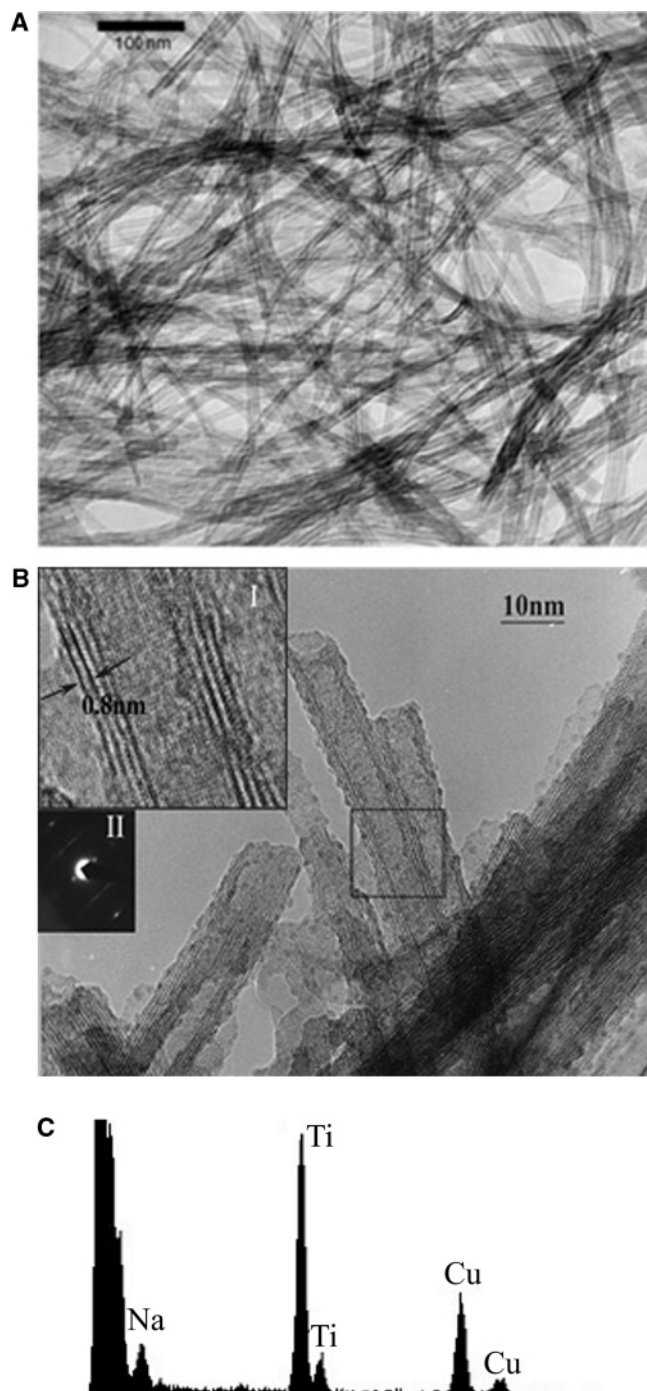


Figure 6. TEM (A), HRTEM (B), and EDXA (C) analyses on sodium titanate nanotubes.³¹

correction resolved an important issue, i.e., which kinds of inorganic compounds can make crystalline nanotubes and which cannot, and meanwhile gave strong support to the “rolling mechanism” because sodium titanates adopt layered structures whereas TiO_2 do not.^{31b}

Because certain amounts of Na or H cations existed between the layered structures, the functionalization of the sodium titanate could be expected by replacing the cations with transition-metal ions, such as Co^{2+} , Ag^+ , etc. The successful synthesis of doped nanotubes explored a simple and effective route to prepare complex metal oxide nanotubes and may have inspired investigations on the chemical,

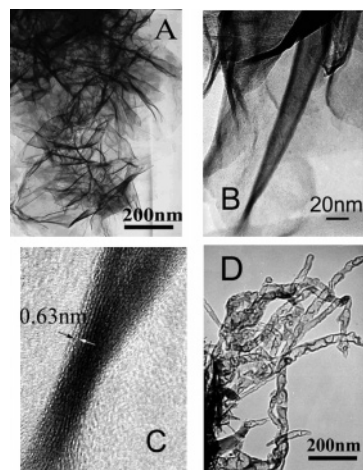


Figure 7. (A) TEM image of the $\alpha\text{-MnO}_2$ intermediate [$(\text{NH}_4)_2\text{S}_2\text{O}_8\text{-MnSO}_4$ reaction system] after hydrothermal treatment for 30 min. (B) HRTEM image of the curling intermediate after hydrothermal treatment for 30 min. (C) HRTEM image of the corresponding part in Figure 3B. (D) TEM image of the $\alpha\text{-MnO}_2$ tubular intermediate after hydrothermal treatment for 45 min.⁵³

physical, and catalytic properties of the complex transition-metal nanoporous materials.

In some cases, compounds with layered structures may serve as intermediates for the formation of nanotubes/nanowires. On the basis of the redox reactions of MnO_4^- and/or Mn^{2+} , a rational low-temperature hydrothermal chemical synthetic mechanism has been developed to selectively prepare MnO_2 nanowires/nanotubes with different crystal structures, including α -, β -, γ -, and δ - MnO_2 .^{51–54} Different forms of MnO_2 are exactly based on the same structural $[\text{MnO}_6]$ octahedral units. α -, β -, and γ - MnO_2 have $[\text{MnO}_6]$ chains in their structures and are typical of 1×1 , 2×2 , and 1×2 1-D channels, respectively, while the δ type is well-known for its layered structure, which is composed of edge-sharing $[\text{MnO}_6]$ octahedra.^{54–59} Among the several crystallographic forms of MnO_2 , δ - MnO_2 alone has a layered structure, which is indispensable in the rolling mechanism. So, studies have been focused on the role that δ - MnO_2 plays in the formation of other structural MnO_2 1-D nanostructures.

Two strategies of Mn^{2+} oxidized into MnO_2 and MnO_4^- reduced into MnO_2 were employed. Although the Mn sources were different, all of the MnO_2 nanowires underwent a similar growing process. For example, the XRD patterns of α - MnO_2 intermediates obtained at shorter reaction time can be readily indexed to that of δ - MnO_2 , and the samples showed lamellar structural morphologies (Figure 7A). When the reaction time was prolonged, lots of nanotubes were observed existing in the intermediate (Figure 7D). However,

(51) Wang, X.; Li, Y. D. *J. Am. Chem. Soc.* **2002**, *124*, 2880–2881.

(52) Wang, X.; Li, Y. D. *Chem. Commun.* **2002**, 764–765.

(53) Wang, X.; Li, Y. D. *Chem.—Eur. J.* **2003**, *9*, 300–306.

(54) Wang, X.; Li, Y. D. *Chem. Lett.* **2004**, *33*, 48–49.

(55) Thackeray, M. M. *Prog. Solid State Chem.* **1997**, *25*, 1–71.

(56) Ching, S.; Welch, E. J.; Hughes, S. M.; et al. *Chem. Mater* **2002**, *14*, 1292–1299.

(57) Ching, S.; Roark, J. L.; Duan, N.; et al. *Chem. Mater.* **1997**, *9*, 750–754.

(58) Ching, S.; Landrigan, J. A.; Jorgensen, M. L.; et al. *Chem. Mater.* **1995**, *7*, 1604–1606.

(59) Armstrong, A. R.; Bruce, P. G. *Nature* **1996**, *381*, 499–500.

after a further prolonged reaction time, the nanotubes disappeared, and only nanowires could be obtained. Meanwhile, the XRD patterns of the samples showed a great similarity to that of α - MnO_2 with less crystallinity.

Similar XRD patterns of δ - MnO_2 were obtained from the intermediate of α - MnO_2 in other reaction systems or the intermediate of δ - MnO_2 . All of the information indicated that they underwent a similar growth process. On the basis of the above experimental results, all of the MnO_2 1-D nanostructures had undergone a common developing process, which was characteristic of the rolling mechanism and phase transformation.

This rolling strategy was further evidenced in the controlled synthesis of δ - MnO_2 nanotubes via α - NaMnO_2 as precursors,⁵⁴ which was layered and adopted a monoclinic distortion of the LiCoO_2 structure caused by the Jahn–Teller activity of Mn^{3+} .^{59,60}

The synthesis of MnO_2 nanowires/nanorods and nanotubes, together with other non-oxide compounds such as Bi nanotubes, shows that a rolling mechanism may be a general way to synthesize nanowires/nanotubes from natural lamellar structures under aqueous conditions. As an example, the successful synthesis of MnO_2 nanowires/nanorods and nanotubes also shows that it is convenient to control the crystal structure or oxidation state of the final products by properly selecting the reaction conditions, which may be the major advantage of a solution-based method.

2. Rare-Earth-Compound Nanotubes and Fullerene-like Nanoparticles.^{61–65} Different from the MnO_2 species, there exist no layered-structure compounds in rare-earth compounds that may serve as intermediates for the formation of 1-D nanostructures. The synthesis of lanthanide hydroxide nanowires was inspired from their crystal structures.⁶¹ As far as the obtained $\text{Ln}(\text{OH})_3$ nanowires ($\text{Ln} = \text{La}, \text{Ce}, \text{Pr}, \text{Nd}, \text{Sm}, \text{Eu}, \text{Gd}, \text{Tb}, \text{Dy}, \text{Ho}, \text{Er}, \text{and Tm}$) were concerned, they all had a hexagonal crystal structure, just like that of ZnO , which was well-known for its anisotropic growth nature. However, during the investigation of the formation process of these nanowires, especially the influence of pH on the morphology evolution of the nanostructures, some sheet structures were obtained (Figure 8A–C) that showed that the hexagonal-structure hydroxides can grow in a 2-D mode under desired conditions.^{61,63,64} So, the question was, can these nontypical 2-D compounds be prepared as nanotubes that were usually prepared from 2-D layered structures? This assumption was confirmed by the formation of hydroxide nanotubes⁶³ under a lower temperature condition than that of nanowires.

The synthesis of $\text{Ln}(\text{OH})_3$ nanowires (Figure 8A–C) was based on the preparation of colloidal $\text{Ln}(\text{OH})_3$ at room

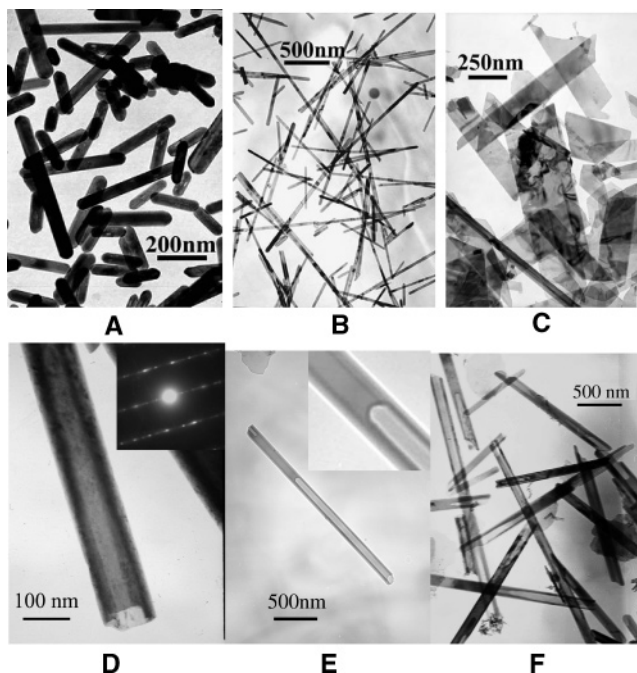


Figure 8. (A) TEM image of $\text{Sm}(\text{OH})_3$ nanosheets, pH = 6–7.⁶¹ (B) TEM image of $\text{Sm}(\text{OH})_3$ nanowires, pH = 9–10.⁶¹ (C) TEM image of $\text{Sm}(\text{OH})_3$ nanorods, KOH, 5 mol/L.⁶¹ (D) TEM image of an individual $\text{Er}(\text{OH})_3$ nanotube with an open end.⁶³ (E) Individual nanotube of $\text{Y}(\text{OH})_3$ containing ethanol.⁶³ (F) TEM image of $\text{Y}(\text{OH})_{2.14}\text{F}_{0.86}$ nanotubes.⁶³

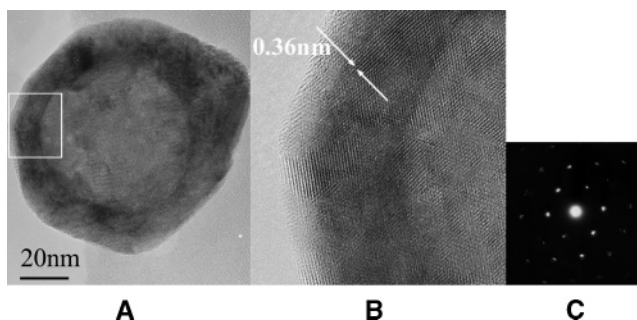


Figure 9. (A) Individual LaF_3 IF nanoparticle with diameter ~ 90 nm. (B) Magnification of the square section shown in part A. (C) Electron diffraction pattern of the IF nanoparticle in part A.⁶²

temperature and the subsequent hydrothermal treatment at 180°C for about 12 h, while the preparation of hydroxide nanotubes (Figure 8D–F) was carried out at lower-temperature conditions from 120 to 140°C . The similar experimental conditions provided an ideal system for the investigation of the formation of nanowires or nanotubes.

Similar precipitation/hydrothermal methods were applied in the synthesis of rare-earth fluoride inorganic fullerene-like (IF) nanoparticles (Figure 9).⁶² Compared with the reported IF/nanotubes nanostructures, rare-earth fluorides and hydroxides had no typical layered structures. However, it seemed that the closed-cage structures were also thermodynamically stable for these fluorides and hydroxides. On the basis of experimental results, we believed that the rare-earth fluorides and hydroxides may not be regarded as typical 3-D compounds and may be the structural intermediates between 3-D and 2-D structures. Similar phenomena were observed and confirmed by Tenne et al. in the subsequent synthesis of nonlayered HfS hollow nanoparticles.⁶⁶ However, a clear

(60) Bach, S.; Pereira-Ramos, J. P.; Baffier, N. *J. Solid State Chem.* **1995**, *120*, 70–73.

(61) Wang, X.; Li, Y. D. *Angew. Chem., Int. Ed.* **2002**, *41*, 4790–4793.

(62) Wang, X.; Li, Y. D. *Angew. Chem., Int. Ed.* **2003**, *42*, 3497–3500.

(63) Wang, X.; Sun, X. M.; Yu, D. P.; Zou, B. S.; Li, Y. D. *Adv. Mater.* **2003**, *15*, 1442–1445.

(64) Wang, X.; Li, Y. D. *Chem.—Eur. J.* **2003**, *9*, 5627–5635.

(65) Wang, X.; Zhuang, J.; Li, Y. D. *Eur. J. Inorg. Chem.* **2004**, *5*, 946–948.

explanation of the structural rational of these IF nanostructures may need a thorough theoretical and structural investigation.

Stemming from an aqueous solution, these hydroxide nanotubes/nanowires were sure to have unique hydrophilic properties and may serve as effective confined templates for 1-D nanostructures (Figure 8E,F). The morphologies of these tubular or nanowire structures can be maintained even after thermal treatment at 700 °C; however, a dehydration process would occur and result in the formation of oxide nanotubes/nanowires. Another treatment mode would lead to the formation of oxysulfide nanotubes/nanowires if the hydroxide ones were mixed with S to form a homogeneous mixture and then treated at a temperature of ~700 °C under the protection of an Ar (N₂) atmosphere. Also, F-substituted hydroxide nanotubes could be prepared. Experiments showed that, based on a simple hydrothermal method and with hydroxides as possible precursors, different kinds of rare-earth-compound nanotubes could be easily obtained, and the great flexibility of rare-earth chemistry was utilized in generating various rare-earth-compound nanomaterials.

The hydrophilic properties of the rare-earth nanotubes/nanowires enabled the possibility of the preparation of inorganic/organic rare-earth nanostructures.⁶⁷ Generally, functional molecules with ester groups can be used in this process. Methyl methacrylate (MMA) was chosen as an example. The covalent functionalization involved the irreversible esterolysis of a bifunctional molecule, MMA, and the formation of Y^{III}—O bonds on the hydrophilic surface of Y(OH)₃ nanotubes in water. This led to amphipathic composite nanotube synthesis by the attachment of C—C double-bond chains to Y(OH)₃ nanotubes without disrupting the original structure.

By effective tuning of the chemical potentials in the aqueous system, a new chemical synthetic strategy was established to synthesize a series of rare-earth nanowires, nanotubes, and IF nanostructures. On the basis of the experimental results, the nanotubes have been obtained at a lower-temperature condition than that of the nanowires, and the structural transitions from rare-earth nanotubes to nanowires have been investigated in detail in different rare-earth systems. A rolling mechanism similar to that of the MnO₂ system has been established to guide the growth of these rare-earth low-dimensional nanostructures, which shows the generality of this mechanism.

3. Rolling Mechanism Based on Organic/Inorganic Lamellar Precursors.^{33,35,37,38} Although we can find many layered structures in the oxides, so far not all of them can be transformed to 1-D nanostructures partly because the interaction between layers may be rather strong and will hold the layers tightly. A general method has been established in the synthesis of WS₂ and VO_x nanotubes and W, WO_{3-x}, and metal nanorods by preliminarily preparing an artificial lamellar structure.

The primary approach was based on self-assembly of inorganic precursors at the template/solution interface using organic molecules as structure-directing agents. The interaction between organic molecules and inorganic precursors could be coordinative interaction,⁶⁸⁻⁷⁰ electrostatic interaction,⁷¹ or even H bonding.⁷² Under certain conditions, the interlayer interaction of these kinds of lamellar intercalates could be diminished from the edges. Then, the rolling of the layers into the tubules would take place. Solution-based routes were rather effective in obtaining various lamellar precursors; however, in some cases they cannot provide enough energy to overcome the interaction between layers from the edges. So, the precursors should be carefully treated under controlled experimental conditions. For example, for the synthesis of WS₂, W, and WO_{3-x} nanotubes/nanorods, a thermal pyrolysis method was developed to convert the lamellar structures into 1-D materials.

The process of designing lamellar precursors and then converting them into 1-D nanostructures via a rolling mechanism can be illustrated with WS₂ as an example.³³

WS₂ nanotubes could be obtained from a direct pyrolysis method from artificial lamellar mesostructures. In this process, a tungsten sulfide artificial lamellar mesostructure composite with intercalated CTA⁺ cations (WS-L) was prepared on the basis of the recently developed template self-assembly of anionic tungstates (WS₄²⁻) and cationic surfactant molecules (CTA⁺) in solution under appropriate conditions. After heating of this inorganic/surfactant lamellar composite material in an Ar atmosphere to 850 °C, bulk quantities of uniform WS₂ nanotubes with diameters of 5–37.5 nm and lengths ranging from 0.2 to 5 μm were produced (Figure 10).

The detailed synthesis process of WS₂ nanotubes was as follows:

Mesolamellar tungsten sulfide (referred to as WS-L) with intercalated CTA⁺ cations was prepared on the basis of a cocondensation mechanism of anionic inorganic species with a cationic surfactant under mild hydrothermal conditions.⁷¹ Then the vacuum pyrolysis carbon thermal (VPC) synthesis of the inorganic/surfactant lamellar (WS-L) precursor was carried out in a conventional tube furnace at elevated temperature from 100 to 850 °C in a high-purity Ar atmosphere (99.999%) with a pressure range of 10⁻²–10⁻³ atm. The whole reaction for the formation of WS₂ nanotubes can be expressed as



The formation mechanism for the synthesis of WS₂ nanotubes was believed to be the general rolling mechanism. It was believed that, under certain conditions, the interlayer

(66) Nath, M.; Rao, C. N. R.; Popovitz-Biro, R.; Albu-Yaron, A.; Tenne, R. *Chem. Mater.* **2004**, *16*, 2238–2243.

(67) Li, W. J.; Wang, X.; Li, Y. D. *Chem. Commun.* **2004**, 164–165.

(68) Antonelli, D. M.; Ying, J. Y. *Angew. Chem., Int. Ed.* **1995**, *34*, 2014–2017.

(69) Antonelli, D. M.; Ying, J. Y. *Angew. Chem., Int. Ed.* **1996**, *35*, 426–430.

(70) Antonelli, D. M.; Ying, J. Y. *Inorg. Chem.* **1996**, *35*, 3126–3136.

(71) Hue, Q. S.; Margolese, D. I.; Ciesla, U.; Feng, P. Y.; Gier, T. E.; Sieger, P.; Leon, R.; Petroff, P. M.; Schuth, F.; Stucky, G. D. *Nature* **1994**, *368*, 317–321.

(72) Tanev, T. T.; Pinnavaia, T. J. *Science* **1995**, *267*, 865–867.

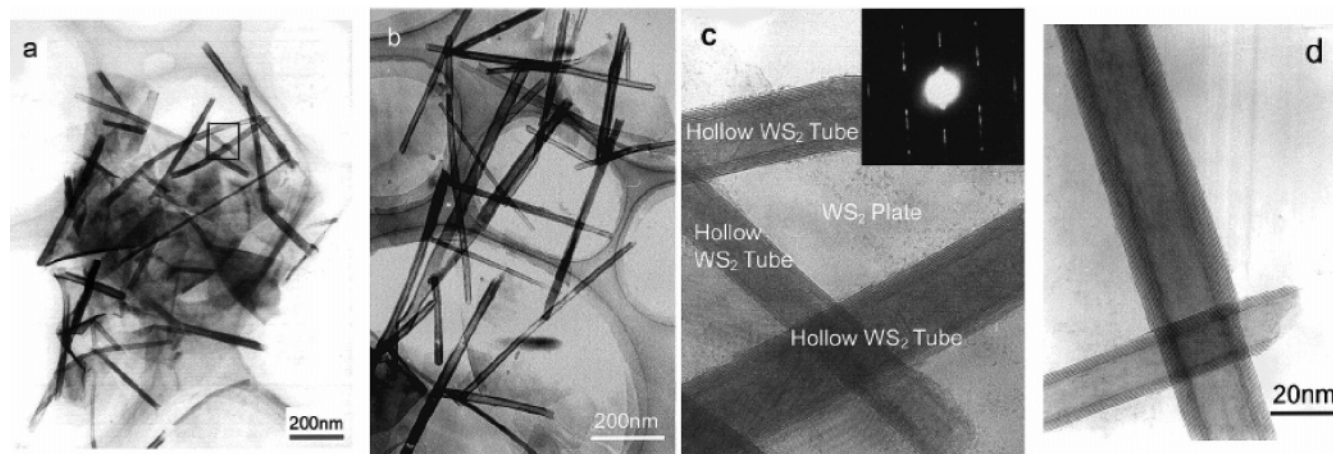


Figure 10. TEM images of the as-synthesized WS_2 nanotubes: (a and b) low-magnification TEM image and (c and d) HRTEM image taken on a JEOL-2010 transmission electron microscope. The area indicated in part a clearly shows the coexistence of hollow WS_2 nanotubes and WS_2 plates. The inset in part c is a SAED pattern taken on an individual nanotube.

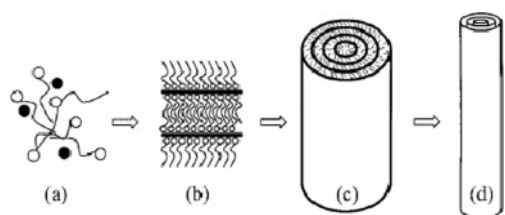


Figure 11. Schematic presentation of the whole rolling mechanism for the formation of WS_2 nanotubes: (a) homogeneous solution of CTA^+ and WS_4^{2-} ; (b) assembly of CTA^+ and WS_4^{2-} into a lamellar structure; (c) rolling of lamellar inorganic/surfactant mesostructures into columnar structures; (d) removal of surfactant molecules and reduction of WS_4^{2-} to form WS_2 nanotubes under VPC conditions.

interaction of this kind of lamellar intercalate could be diminished from the edges and the layers rolled into tubules. Transformation of these tubules into WS_2 nanotubes could be realized through removal of the organic surfactants and reduction of WS_4^{2-} to WS_2 . The scheme for the formation of nanotubes could be divided into four steps: (i) The CTAB surfactant molecules were condensed into aggregations with WS_4^{2-} anions intercalated into the interspaces between the headgroups of CTAB to form CTA/WS_4 ion pairs. (ii) The condensation process was continued and brought out more ordered lamellar assemblies. (iii) When heated in a vacuum at gradually elevated temperature, these lamellar sheets began to loosen at the sheet edge and then rolled into separate scrolls, which were a combination of CTA^+ cations and WS_4^{2-} anions. (iv) With increasing furnace temperature, in situ reduction of WS_4^{2-} by the pyrolyzed C from CATB happened and thus produced WS_2 with a morphology confined by the scrolls, which might serve as microreactors in the VPC process and were responsible for the ultimate formation of tubular WS_2 (Figure 11).

This mechanism was firmly grounded in experimental observations. The most direct evidence of the rolling of WS_2 layers to form nanotubes was the demonstration of a half-rolled structure (Figure 12), with a perfect tubular structure at one end (parts A and B) and a sheetlike structure at the initial stage of rolling at the other end (parts C and D). Actually, high temperature or thermal stress may initiate bending of the layered structures, with or without the aid of

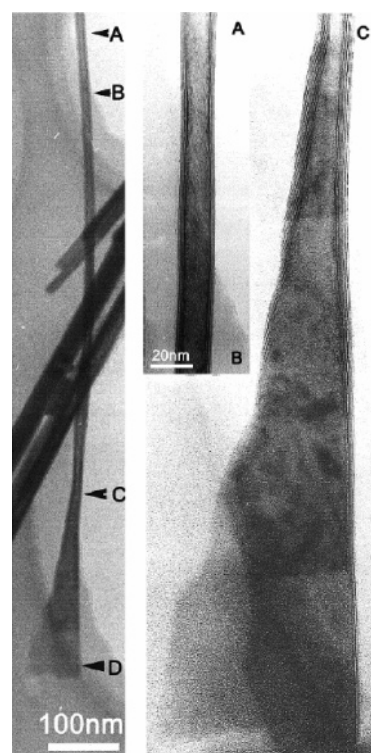


Figure 12. TEM image of a half-tube and half-plate structure. D \rightarrow C \rightarrow B \rightarrow A shows the transition from a platelike structure to a tubular structure.

intercalations. Severe bending of the graphite sheets at high temperature was a common phenomenon,⁷³ and curling of graphitic networks was observed under electron beam irradiation.⁷⁴

Following a similar rolling process, W^{37} and WO_{3-x} ³⁸ nanowires can also be obtained if mesolamellar composites of tungsten oxide with CTA^+ surfactant cations (WO-L) were adopted. In the case of W nanowires, a vacuum carbon thermal reduction method was adopted, while thermal treatment of these precursors led to the formation of WO_{3-x} nanorods. Because W and WO_{3-x} had no layered structure

(73) Heidenreich, R. D.; Hess, W. M.; Ban, L. L. *J. Appl. Crystallogr.* **1968**, *1*, 1.

(74) Ugarte, D. *Nature* **1992**, *359*, 707.

in nature, nanotubes were not their stable forms, and after a rolling process, the lamellar precursors would collapse into nanowires or nanorods, in a way similar to that of MnO₂ nanowires.

The self-assembly process between surfactants and metal ions was quite general, and a broad range of organic/inorganic lamellar composites can be easily obtained. On the basis of these assembly processes and vacuum carbon thermal reduction treatment, a novel and relatively simple synthesis method for oxide and metal nanowires was developed. These demonstrated that the rolling mechanism may be a general mechanism for growth of nanotubes/nanorods from a layered structure, and it was expected that a general synthetic method of nanotubes may be developed based on this mechanism.

In some cases, hydrothermal treatment would provide enough energy for the lamellar precursors to roll into scroll-type nanotubes. In these nanotubes, the surfactants were not removed and resided between the inorganic layers. A typical example was the synthesis of VO_x nanotubes (VO_x-NTs).

VO_x-NTs were first synthesized by Nesper and co-workers in a sol-gel reaction followed by hydrothermal treatment from vanadium alkoxide precursors and primary amines.^{75,76} This process involved an intermediate artificial lamellar composite of the surfactant and the VO_x, the hydrolysis product of a vanadium alkoxide precursor in the presence of hexadecylamine. These lamellar structures then rolled into VO_x nanotubes along with the intercalated amine in hydrothermal conditions. The distance between the layers in the VO_x nanotubes can be controlled by the length of the -CH₂- chain in the amine template. By an alternative approach,³⁵ using NH₄VO₃ instead of vanadium alkoxide as the starting material, VO_x-NTs were also obtained in large quantities.

In these compounds, the surfactants were coordinatively (amines) or electrostatically bound (ammoniums) via their headgroups to discrete inorganic precursor units (VO₃⁻). Then relatively stable organic/inorganic-layered structures could be formed with the surfactants intercalated between VO₅. Considering the generality of the reactant and surfactants, the formation mechanism of this kind of artificial lamellar structure may be generally applied, which is critical for a general synthetic mechanism.

There were more examples of the "rolling mechanism". In the earlier work of Domen and Mallouk and co-workers on the chemical transformation of lamellar oxides into single-sheet colloids, tubular structures, and unilamellar sheets, the rolling phenomenon was also observed and interpreted, which also revealed the possibility for a lamellar sheet to form a tubular structure through a similar rolling process.⁷⁷⁻⁷⁹ Remskar and co-workers obtained direct evidence for the

derivation of tubules from the bending of platelets.⁸⁰⁻⁸² Yada et al. reported the formation of tubular structures through the folding of flexible Al-based layers.⁸³ Kaner et al. reported the synthesis of C nanoscrolls by a chemical route.⁸⁴ All of these results have undoubtedly verified the proposed rolling mechanism and indicate that this process is general for the synthesis of 1-D nanostructures.

Part III. Controlled Growth of Nanowires/Nanorods Based on Anisotropic Crystal Structures

Another important strategy is that crystal structures with a preferential axis may be preferable for the growth of nanowires; for example, hexagonal ZnO, Mg(OH)₂, and lanthanide hydroxide nanowires have been successfully synthesized through a hydrothermal/solvothermal synthetic mechanism. A closer look over the inherent crystal structure may help us to judge the possibilities of preparing 1-D nanostructures. Particularly, rare-earth compounds may serve as a perfect model to study the crystallization in nanoscale because they have similar and gradually changing crystal structures.

As mentioned above, most of the lanthanide hydroxides have hexagonal crystal structures, just like that of ZnO, which is well-known for its anisotropic growth nature.

It was interesting to find that, under controlled experimental conditions, the different light Ln(OH)₃ [La(OH)₃, Pr(OH)₃, Nd(OH)₃, Sm(OH)₃, Eu(OH)₃, and Gd(OH)₃] nanowires could be prepared as high-aspect-ratio products with similar outlook, while under the same conditions, heavier lanthanide hydroxides [Dy(OH)₃, Tb(OH)₃, Ho(OH)₃, Tm(OH)₃ and YbOOH] usually had lower aspect ratios or less uniform morphologies.⁶¹

With a decrease of the ionic radii (from La to Lu),⁸⁵ under the adopted experimental conditions, the crystal structure of lanthanide hydroxides gradually changed from a typical hexagonal phase [La(OH)₃] to a monoclinic one [Lu(OH)₃], which resulted in the formation of monoclinic YbOOH instead of hexagonal Yb(OH)₃ in high-temperature (nanowire synthesis, 180 °C) experimental conditions; along with this change, the tendency to grow along a certain direction was weakened to some extent, so the heavier lanthanide hydroxide nanowires usually had lower aspect ratios and less uniform morphologies.

Similar phenomena were observed in the controlled synthesis of LnPO₄ nanowires.⁸⁶ Lanthanide phosphates derived under identical synthesis conditions adopted three different crystal structures. Although the exact reason for

(75) Krumeich, F.; Muhr, H. J.; Niederberger, M.; Bieri, F.; Schnyder, B.; Nesper, R. *J. Am. Chem. Soc.* **1999**, *121*, 8324-8331.

(76) Spahr, M. E.; Bitterli, P.; Nesper, R.; Muller, M.; Krumeich, F.; Nissen, H. U. *Angew. Chem., Int. Ed.* **1998**, *37*, 1263-1265.

(77) Abe, R.; Shinohara, K.; Tanaka, A.; Hara, M.; Kondo, J.; Domen, K. *Chem. Mater.* **1997**, *9*, 2179-2184.

(78) Saupé, G. B.; Waraksa, C. C.; Kin, H. N.; Han, Y. J.; Kaschak, D. M.; Skinner, D. M.; Mallouk, T. E. *Chem. Mater.* **2000**, *12*, 1556-1562.

(79) Schaak, R. E.; Mallouk, T. E. *Chem. Mater.* **2000**, *12*, 3427-3434.

(80) Remskar, M.; Skraba, Z.; Cleton, F.; Sanjines, R.; Levy, F. *Appl. Phys. Lett.* **1996**, *69*, 351-353.

(81) Remskar, M.; Skraba, Z.; Regula, M.; Ballif, C.; Sanjines, R.; Levy, F. *Adv. Mater.* **1998**, *10*, 246-249.

(82) Remskar, M.; Skraba, Z.; Sanjines, R.; Levy, F. *Appl. Phys. Lett.* **1999**, *74*, 3633-3635.

(83) Yada, M.; Hiyoshi, H.; Ohe, K.; Machida, M.; Kijima, T. *Inorg. Chem.* **1997**, *36*, 5565-5569.

(84) Viculis, L. M.; Mack, J. J.; Kaner, R. B. *Science* **2003**, *299*, 1361-1361.

(85) Huang, C. H. *Rare Earth Coordination Chemistry*; Science Press: Beijing, 1997; p 25.

(86) Yan, R. X.; Sun, X. M.; Wang, X.; Peng, Q.; Li, Y. D. *Chem.-Eur. J.* **2005**, *11*, 2183-2195.

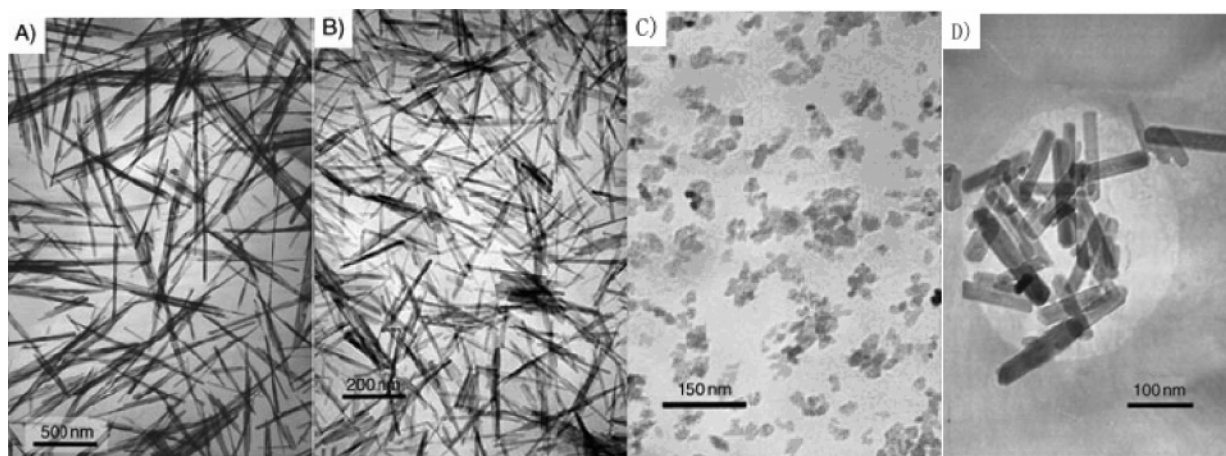


Figure 13. (A) TEM image of LaPO_4 nanowires. (B) TEM image of $\text{SmPO}_4 \cdot 0.5\text{H}_2\text{O}$ nanowires. (C) TEM image of YPO_4 nanoparticles (180°C , 0.1 g of EDTA). (D) TEM image of YPO_4 nanoparticles (180°C , 0.5 g of EDTA).

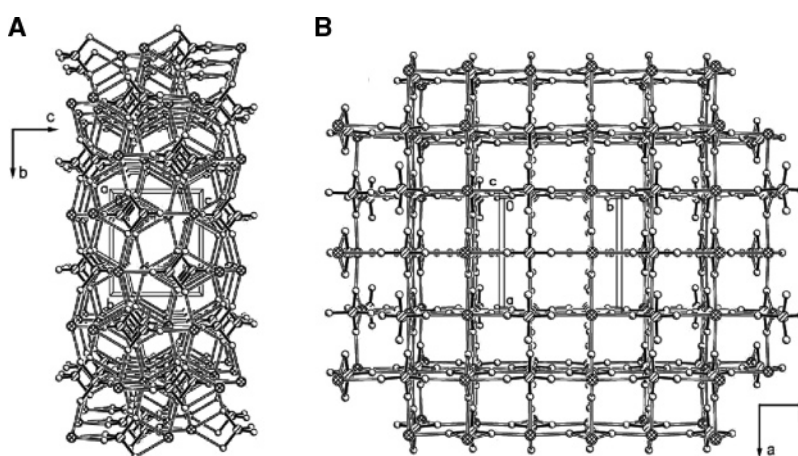


Figure 14. (A) Perspective view along the a axis of the molecular packing of HoPO_4 . (B) Perspective view along the c axis of the molecular packing of HoPO_4 (dashed circle = P, open circle = O, crossed circle = Ho).

this phenomenon was not yet clearly known, the switches of the crystal structure seemed to be closely related to the gradual contraction of the Ln^{3+} radius. Generally, for larger Ln^{3+} , a monoclinic structure was preferred. For Ln^{3+} of intermediate size, a partly hydrated hexagonal structure was more favorable. For the smaller heavy Ln^{3+} ions, a tetragonal phase was adopted. Except in the monoclinic phase, where the coordination number of Ln^{3+} was 9, Ln^{3+} in both the hexagonal and tetragonal phases was eight-coordinate because, as the radius of the Ln^{3+} decreased, the accommodation of an extra coordinating O atom became increasingly difficult.

All of the monoclinic LnPO_4 (Figure 13A) and hexagonal $\text{LnPO}_4 \cdot n\text{H}_2\text{O}$ products (Figure 13B) displayed a uniform rodlike morphology with a length in the range of 0.3–3 μm and a width in the range of 10–100 nm. However, under the same synthetic conditions, the tetragonal LnPO_4 ($\text{Ln} = \text{Dy} - \text{Lu}$ and Y) crystals exhibited spherulike morphology (Figure 13C). It was apparent that, compared with the monoclinic and hexagonal LnPO_4 compounds, the anisotropic growth tendency of the tetragonal ones was comparatively weak. However, a more careful examination of the crystal structure of the tetragonal LnPO_4 suggested that the (110)

facet bore more dangling bonds and that growth along the (110) direction released more energy, thus making the (110) facet of higher chemical potential than the (100), (010), and (001) facets (Figure 14). This special feature of the (110) facet of this tetragonal structure may shed some light on the anisotropic nature of heavy lanthanide phosphates, although the tendency for anisotropic growth of these tetragonal LnPO_4 may not be as strong as that of their monoclinic and hexagonal counterparts, as indicated by the experimental results. However, under suitable synthetic conditions, the intrinsic anisotropic feature of tetragonal LnPO_4 may be magnified, leading to the formation of 1-D nanostructures. Peng and Peng⁸⁷ showed that 1-D growth only occurred if the chemical potential of the monomers in solution was much higher than the highest chemical potential of the atoms on the surface of the nanocrystals. This concept was extensively demonstrated in hydrothermal syntheses of various 1-D nanostructures. It was also reasonable to assume that oriented growth of the tetragonal LnPO_4 can be ensured by modifying the composition of the solution such that the chemical potential of the monomer was maximized. On the basis of

(87) Peng, Z. A.; Peng, X. G. *J. Am. Chem. Soc.* **2001**, *123*, 1389–1395.

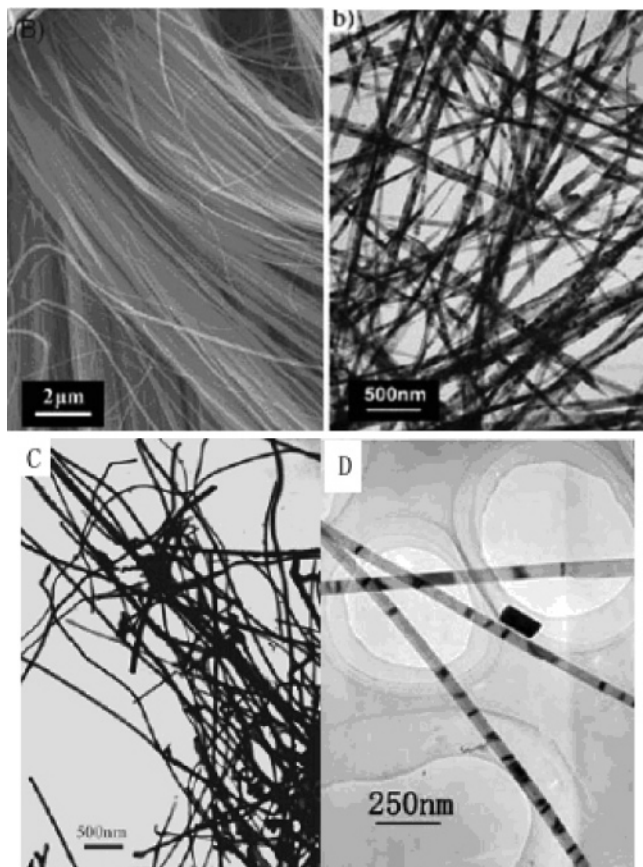


Figure 15. (A) Typical field emission scanning electron microscopy image of $V_2O_5 \cdot xH_2O$ nanobelts.⁸⁸ (B) TEM image of VO_2 nanobelts.⁸⁷ (C) TEM image of Bi nanowires.⁹⁰ (D) TEM image of Bi_3O_4Br nanobelts.⁸⁹

these analyses, the growth of tetragonal $LnPO_4$ nanorods was achieved (Figure 13D) by using ethylenediaminetetraacetic acid (EDTA) as a complex reagent for Ln^{3+} .

On the basis of the experimental results on the rare-earth-compound nanowires, it can be concluded that 1-D nanostructures of highly anisotropic polymorphs (hexagonal) could be synthesized simply by adjusting the acidity of the stock solution. For compounds such as tetragonal $LnPO_4$, only irregularly shaped particles could be obtained under similar synthetic conditions. However, on the basis of intrinsic anisotropy of the crystal structure, the anisotropic growth of these compounds can be realized by varying the chemical potentials of the species in solution through the use of chelating ligands. This successful demonstration may assist us in understanding the fundamentals of the reaction and of nanowire growth mechanisms under solution-based conditions.

The syntheses of many kinds of other 1-D nanostructures were achieved via solution-based methods, including VO_2 ⁸⁸ and VO_x ⁸⁹ nanowires, $BrOBr$,⁹⁰ Bi,⁹¹ and $BrOCl$ ⁹² nanobelts (Figure 15), etc. For all of these 1-D nanostructures, a deep understanding of their crystal structure greatly help in choosing the appropriate conditions.

Summary and Perspective

This Forum Article provides an overview of the research progress in our laboratory on solution-based routes to 1-D nanostructures. Crystal structure as one of the inherent factors that may determine the growth behavior of nanocrystals is emphasized, and particularly compounds with layered structures or anisotropic crystal structures are given special attention. The direct correlation between the crystal structure and growth behavior of materials will contribute greatly to the precise control over sizes, dimensionalities, compositions, and crystal structures in nanoscale as well as the tailoring of physical/chemical properties of materials in a controllable way and thus deserves more investigation.

The inorganic nanowires/nanotubes have shown vivid images for their applications in the future. The unique electronic properties of nanotubes/nanowires are of significant importance in future nanoelectronics. Meanwhile, morphology-controlled synthesis of single-crystal 1-D nanostructures may represent an opportunity for the synthesis of a highly reactive/selective catalyst because these novel materials expose defined crystal planes. We can expect that the synthesis of new inorganic nanowires/nanotubes and their scientific interests and industrial applications will stimulate researches such as electronics, mechanics, biology, and medicine.

Acknowledgment. This work was supported by NSFC (Grants 20501013, 50372030, 20131030, and 90406003), the Foundation for the Author of National Excellent Doctoral Dissertation of the People's Republic of China, and the State Key Project of Fundamental Research for Nanomaterials and Nanostructures (Grant 2003CB716901).

IC0518850

- (88) Liu, J. F.; Li, Q. H.; Wang, T. H.; Yu, D. P.; Li, Y. D. *Angew. Chem., Int. Ed.* **2004**, *43*, 5048–5052.
 (89) Liu, J. F.; Wang, X.; Peng, Q.; Li, Y. D. *Adv. Mater.* **2005**, *17*, 764–767.
 (90) Wang, J. W.; Li, Y. D. *Chem. Commun.* **2003**, 2320–2321.
 (91) Wang, J. W.; Wang, X.; Peng, Q.; Li, Y. D. *Inorg. Chem.* **2004**, *43*, 7552–7556.
 (92) Deng, H.; Wang, J. W.; Peng, Q.; Wang, X.; Li, Y. D. *Chem.—Eur. J.* **2005**, *11*, 6519–6524.